NASA/TM—2000-107249/Chapter 6

Solid Lubrication Fundamentals and Applications

Friction and Wear Properties of Selected Solid Lubricating Films: Case Studies

Kazuhisa Miyoshi
Glenn Research Center, Cleveland, Ohio

December 2000

The NASA STI Program Office . . . in Profile

Since its founding, NASA has been dedicated to the advancement of aeronautics and space science. The NASA Scientific and Technical Information (STI) Program Office plays a key part in helping NASA maintain this important role.

The NASA STI Program Office is operated by Langley Research Center, the Lead Center for NASA's scientific and technical information. The NASA STI Program Office provides access to the NASA STI Database, the largest collection of aeronautical and space science STI in the world. The Program Office is also NASA's institutional mechanism for disseminating the results of its research and development activities. These results are published by NASA in the NASA STI Report Series, which includes the following report types:

- TECHNICAL PUBLICATION. Reports of completed research or a major significant phase of research that present the results of NASA programs and include extensive data or theoretical analysis. Includes compilations of significant scientific and technical data and information deemed to be of continuing reference value. NASA's counterpart of peer-reviewed formal professional papers but has less stringent limitations on manuscript length and extent of graphic presentations.

- TECHNICAL MEMORANDUM. Scientific and technical findings that are preliminary or of specialized interest, e.g., quick release reports, working papers, and bibliographies that contain minimal annotation. Does not contain extensive analysis.

- CONTRACTOR REPORT. Scientific and technical findings by NASA-sponsored contractors and grantees.

- CONFERENCE PUBLICATION. Collected papers from scientific and technical conferences, symposia, seminars, or other meetings sponsored or cosponsored by NASA.

- SPECIAL PUBLICATION. Scientific, technical, or historical information from NASA programs, projects, and missions, often concerned with subjects having substantial public interest.

- TECHNICAL TRANSLATION. English-language translations of foreign scientific and technical material pertinent to NASA's mission.

Specialized services that complement the STI Program Office's diverse offerings include creating custom thesauri, building customized data bases, organizing and publishing research results . . . even providing videos.

For more information about the NASA STI Program Office, see the following:

- Access the NASA STI Program Home Page at ***http://www.sti.nasa.gov***

- E-mail your question via the Internet to help@sti.nasa.gov

- Fax your question to the NASA Access Help Desk at 301–621–0134

- Telephone the NASA Access Help Desk at 301–621–0390

- Write to:
  NASA Access Help Desk
  NASA Center for AeroSpace Information
  7121 Standard Drive
  Hanover, MD 21076

NASA/TM—2000-107249/Chapter 6

Solid Lubrication Fundamentals and Applications

Friction and Wear Properties of Selected Solid Lubricating Films: Case Studies

Kazuhisa Miyoshi
Glenn Research Center, Cleveland, Ohio

National Aeronautics and
Space Administration

Glenn Research Center

December 2000

Available from

NASA Center for Aerospace Information
7121 Standard Drive
Hanover, MD 21076
Price Code: A03

National Technical Information Service
5285 Port Royal Road
Springfield, VA 22100
Price Code: A03

Available electronically at http://gltrs.grc.nasa.gov/GLTRS

Chapter 6
Friction and Wear Properties of Selected Solid Lubricating Films: Case Studies

6.1 Introduction

Once the initial shortcomings relating to friction, wear, and lubrication in design and application had been dealt with, it became increasingly clear that materials science and technology ranked equal with design in reducing the friction and wear of machinery and mechanical components [6.1]. This conclusion applied particularly in the field of solid lubrication of aerospace mechanisms.

In modern technology the coefficient of friction and the wear rate are regarded as widely variable, depending on lubricants, operational variables, substrate properties, and surface films. Therefore, testing is central and of great importance to tribologists, lubrication specialists, designers, and engineers. Particularly, standard performance testing of solid lubricant systems is important for the lubricant manufacturer during development of new lubricating materials, for quality control of lubricant manufacture, and for providing quantitative criteria for manufacturing specifications.

Compiling manufacturers' standard test results for a number of lubricant formulations can aid mechanism design engineers (i.e., users) in selecting the best lubricant for an application. However, such data can at best only narrow the field to a specific class of lubricants. Deciding on the optimum lubricant formulation for a specific application requires more custom-design, element, component, and full-scale testing. However, after the optimum lubricant has been chosen, such standard tests can also be useful for quality control. This is especially important in a long space program where satellites or launch vehicles are built over a period of years during which lubricant formulations and film application procedures might undergo change. For solid lubricant films the end user should request that standard test coupons be coated along with the actual parts. Testing each lubricant batch will ensure that the manufacturing quality remains constant throughout the life of the program.

The technology of solid lubrication has advanced rapidly in the past four decades, responding primarily to the needs of the automobile and aerospace industries. Solid

lubrication can be accomplished in several modes: lubricating powders, bonded films, lubricant composites (metal and plastic based), and lubricating coatings and films. This chapter, however, primarily describes bonded films and lubricating coatings and films.

6.2 Commercially Developed Dry Solid Film Lubricants

This section is limited to discussing the tribological properties, particularly friction and wear, of the solid lubricating films selected from commercially developed, affordable dry solid film lubricants (Table 6.1):

1. Bonded molybdenum disulfide (MoS_2), the most widely used mode
2. Magnetron-sputtered MoS_2
3. Ion-plated silver
4. Ion-plated lead
5. Magnetron-sputtered diamondlike carbon (MS DLC)
6. Plasma-assisted, chemical-vapor-deposited diamondlike carbon (PACVD DLC)

The friction and wear properties of the selected solid lubricating films were examined in ultrahigh vacuum, in humid air at a relative humidity of ~20%, and in dry nitrogen at a relative humidity of <1%. Unidirectional pin-on-disk sliding friction experiments were conducted with AISI 440C stainless steel balls in sliding contact with the solid lubricating films at room temperature in the three environ-

TABLE 6.1.—CHARACTERISTICS OF SELECTED SOLID LUBRICATING FILMS
[Substrate material, 440C stainless steel.]

Film	Film material	Film thickness, μm	Film surface roughness,[a] R_a, nm	
			Mean	Standard deviation
Bonded MoS_2	MoS_2, polyimide-imide, others (proprietary blend)	10±4	1.2×10^3	2.4×10^2
MS MoS_2	MoS_2	1.0±0.2	32	4.0
Ion-plated silver	Silver	0.5±0.2	30	3.2
Ion-plated lead	Lead	0.55	98	15
MS DLC	Carbon and WC	2 to 3	43	5.1
PACVD DLC	Carbon and Si	3 to 5	29	3.2

[a]The centerline-average roughness R_a was measured by using a cutoff of 1 mm.

ments. The resultant solid lubricating films and their wear surfaces were characterized by scanning electron microscopy (SEM), energy-dispersive x-ray spectroscopy (EDX), and surface profilometry. SEM and EDX were used to determine the morphology and elemental composition of wear surfaces and wear debris. The sampling depth of EDX for elemental information ranged between 0.5 and 1 μm. Surface profilometry was used to determine the surface morphology, roughness, and wear of the films.

6.2.1 Selected Solid Lubricating Films

Molybdenum disulfide films.—The technical use of molybdenum disulfide as a lubricating solid started in the 1940's. It is now used in more applications than any other lubricating solid. MoS_2 differs from graphite mainly in that its low friction is an inherent property and does not depend on the presence of adsorbed vapors [6.2]. Therefore, it can be used satisfactorily in both high vacuum and dry environmental conditions and has been used in many spacecraft applications. For example, the extendible legs on the Apollo lunar module were lubricated with bonded MoS_2. It is usable at low temperatures and to 350 °C in air or 1000 °C in high vacuum with high load-carrying capacity. At 350 °C in air MoS_2 begins to oxidize. Apart from oxidation it is stable with most chemicals but is attacked by strong oxidizing acids and by alkalis. MoS_2 is a poor conductor of heat and electricity and stable in vacuum.

A useful MoS_2 film can be obtained by

1. Simply rubbing or burnishing MoS_2 powder onto a substrate material
2. Dipping, brushing, or spraying with a dispersion of MoS_2 in a volatile solvent or water and allowing the liquid to evaporate
3. Using a binder material (resin, silicate, phosphate, or ceramic)
4. Vacuum sputtering

Bonded films are much thicker than sputtered films and much more readily available. Sputtered films are easier to incorporate in precision bearing systems. On the whole, MoS_2 is a versatile and useful solid lubricant [6.2–6.4].

The bonded MoS_2 films studied were relatively rough with centerline-average roughness R_a of 1.2 μm, and the magnetron-sputtered MoS_2 films studied were relatively smooth with R_a in the range of 32 nm [6.5]. The bonded films were 10 times thicker than the sputtered films.

Silver and lead films.—Soft metals like silver and lead can be sheared easily and have a number of other properties that make them attractive as solid lubricants for certain circumstances or special situations. For example, in addition to their low shear strengths and ability to be applied as continuous films over harder substrates, soft metals are good conductors of heat and electricity and are stable in vacuum or when exposed to nuclear radiation [6.6].

Soft metal films can be deposited as lubricating films on harder substrates by conventional electroplating or by physical vapor deposition methods such as evaporation, vacuum sputtering, and ion plating. Ion plating and vacuum sputtering permit close control of film deposition and thickness and can provide good adhesion to the substrate [6.7]. Soft metal films are usually about 0.25 to 1.0 μm thick and must be very smooth and uniform. Friction increases with either thicker or thinner films [6.8].

Thin-metal-film lubrication is most relevant at high temperatures or in applications where sliding is limited (e.g., rolling-element bearings). Silver and barium films have been used successfully on lightly loaded ball bearings in high-vacuum x-ray tubes. Silver and gold films have been tested successfully for high-vacuum use in spacecraft applications. Perhaps the most successful applications so far have used thin lead films as long-term, rolling-element (ball) bearing lubrication in spacecraft [6.2, 6.9]. One advantage of lead films over silver or indium is the unavoidable presence of lead oxide (PbO), a reputedly good solid lubricant, within the films [6.1, 6.10]. Ion-plated lead films are used in such mechanisms as solar array drives in European satellites [6.11]. Lead films have been used for many years to lubricate rolling-element bearings on rotating anode x-ray tubes, on satellite parts operating in space, and on other equipment exposed to high temperatures and nuclear radiation. Gold-, silver-, and lead-coated, rolling-element bearings are commercially available at reasonable prices.

The ion-plated silver and ion-plated lead films studied [6.5, 6.12] were relatively smooth with R_a of 30 and 98 nm, respectively, and ~0.5 μm thick and uniform.

Diamondlike carbon films.—A new category of solid lubricants and lubricating films, diamond and related hard materials, is continuing to grow. Particularly, mechanical parts and components coated with diamondlike carbon (DLC) are of continuously expanding commercial interest.

DLC can be divided into two closely related categories: amorphous, non-hydrogenated DLC (a-DLC or a-C) and amorphous, hydrogenated DLC (H–DLC or a-C:H) [6.8]. H–DLC contains a variable and appreciable amount of hydrogen. DLC can be considered a metastable carbon produced as a thin film with a broad range of structures (primarily amorphous with variable sp^2/sp^3 bonding ratio) and compositions (variable hydrogen concentration). A DLC's properties can vary considerably as its structure and composition vary [6.13–6.17]. Although it is a complex engineering job, it is often possible to control and tailor the properties of a DLC to fit a specific application and thus ensure its success as a tribological product. However, such control demands a fundamental understanding of the tribological properties of DLC films. The absence of this understanding can act as a brake in applying DLC to a new product and in developing the product.

Commercial applications of DLC, as protecting, self-lubricating coatings and films, are already well established in a number of fast-growing industries [6.18–6.20] making

1. Magnetic recording media and high-density magnetic recording disks and sliders (heads)
2. Process equipment (e.g., digital video camcorders and copy machines)
3. Abrasion-resistant optical products, rubbers, and plastics
4. Implant components including hip and knee joints, blood pumps, and other medical products
5. Packaging materials and electronic devices
6. Forming dies (e.g., plastic molds and stamping devices)
7. Blades (e.g., razor blades and scalpels)
8. Engine parts (e.g., cam followers, pistons, gudgeon pins, and gear pumps)
9. Mechanical elements (e.g., washers, such as grease-free ceramic faucet valve seats; seals; valves; gears; bearings; bushing tools; and wear parts)

The cost is affordable and generally similar to that of carbide or nitride films deposited by chemical or physical vapor deposition (CVD or PVD) techniques [6.13]. The surface smoothness, high hardness, low coefficient of friction, low wear rate, and chemical inertness of DLC coatings and films, along with little restriction on geometry and size, make them well suited as solid lubricants combating wear and friction.

The magnetron-sputtered (MS) DLC films and plasma-assisted (PA) CVD DLC films studied were relatively smooth with R_a of 43 and 29 nm, respectively, and ~2 to 5 μm thick and uniform [6.21]. The MS DLC films had a multilayer structure and were prepared by using two chromium targets, six tungsten carbide (WC) targets, and methane (CH_4) gas. The multilayer film had alternating 20- to 50-nm-thick WC and carbon layers. The Vickers hardness number was ~1000. The PACVD DLC films were prepared by using radiofrequency plasma and consisted of two layers, an ~2-μm-thick DLC layer on an ~2-μm-thick silicon-DLC underlayer. The DLC top layer was deposited by using CH_4 gas at a total pressure of 8 Pa with a power of 1800 to 2000 W at –750 to –850 V for 120 min. The silicon-containing DLC underlayer was deposited by using a mixture of CH_4 and tetramethylsilane ($C_4H_{12}Si$) gases. The ratio of the concentration of CH_4 and $C_4H_{12}Si$ used was 90:18 (std cm^3/min) at a total pressure of 10 Pa with a power of 1800 to 2000 W at –850 to –880 V for 60 min. The Vickers hardness number was 1600 to 1800.

The 6-mm-diameter 440C stainless steel balls (grade 10) used were smooth, having R_a of 6.8 nm with a standard deviation of 1.8 nm.

6.2.2 Comparison of Steady-State Coefficients of Friction and Wear Rates

Table 6.2 and Figs. 6.1 to 6.3 summarize the steady-state coefficients of friction, the wear rates (dimensional wear coefficients) for the solid lubricating films, and the wear rates for the 440C stainless steel balls after sliding contact in all three environments: ultrahigh vacuum, humid air, and dry nitrogen. The data presented

TABLE 6.2.—STEADY-STATE COEFFICIENT OF FRICTION, WEAR LIFE, AND WEAR RATE FOR SELECTED SOLID LUBRICATING FILMS IN SLIDING CONTACT WITH 440C STAINLESS STEEL BALLS

Film	Environment	Steady-state coefficient of friction	Film wear (endurance) life[a]	Film wear rate, $mm^3/N \cdot m$	Ball wear rate, $mm^3/N \cdot m$
Bonded MoS_2	Vacuum	0.045	>1 million	6.0×10^{-8}	1.3×10^{-9}
	Air	0.14	113 570	2.4×10^{-6}	8.1×10^{-8}
	Nitrogen	0.04	>1 million	4.4×10^{-8}	6.9×10^{-10}
MS MoS_2	Vacuum	0.070	274 130	9.0×10^{-8}	2.5×10^{-9}
	Air	0.10	277 377	2.4×10^{-7}	1.5×10^{-7}
	Nitrogen	0.015	>1 million	1.6×10^{-8}	9.9×10^{-10}
Ion-plated silver	Vacuum	0.20	364 793	8.8×10^{-8}	2.4×10^{-8}
	Air	0.43	8	5.5×10^{-5}	1.2×10^{-5}
	Nitrogen	0.23	1040	1.6×10^{-5}	1.6×10^{-5}
Ion-plated lead	Vacuum	0.15	30 294	1.5×10^{-6}	7.6×10^{-7}
	Air	0.39	82	3.7×10^{-6}	3.6×10^{-7}
	Nitrogen	0.48	1530	9.1×10^{-6}	3.4×10^{-6}
MS DLC	Vacuum	0.70	<10	5.7×10^{-5}	3.2×10^{-4}
	Air	0.12	>1 million	1.7×10^{-7}	4.1×10^{-8}
	Nitrogen	0.12	23 965	4.2×10^{-7}	1.1×10^{-7}
PACVD DLC	Vacuum	0.54	<10	1.1×10^{-5}	1.8×10^{-4}
	Air	0.07	>1 million	1.0×10^{-7}	2.3×10^{-8}
	Nitrogen	0.06	>1 million	1.1×10^{-8}	6.4×10^{-9}

[a]Film wear life was determined to be the number of passes at which the coefficient of friction rose to 0.30.

in the table reveal the marked differences in friction and wear resulting from the environmental conditions and the solid lubricating film materials.

Ultrahigh vacuum.—In sliding contact with 440C stainless steel balls in ultrahigh vacuum, the bonded MoS_2 films had the lowest coefficient of friction, lowest film wear rate, and lowest ball wear rate (Fig. 6.1). The MS MoS_2 films also had low coefficient of friction, low film wear rate, and low ball wear rate, similar to those for the bonded MoS_2. The wear rates of the solid lubricating films and the counterpart steel balls in ultrahigh vacuum were, in ascending order, bonded MoS_2 < MS MoS_2 < ion-plated silver < ion-plated lead < PACVD DLC < MS DLC. The coefficients of friction were in a similar ascending order. The MS DLC films had the highest coefficient of friction, the highest film wear rate, and the highest ball wear rate in ultrahigh vacuum.

Humid air.—In sliding contact with 440C stainless steel balls in humid air, the PACVD DLC films had the lowest coefficient of friction, lowest film wear rate, and lowest ball wear rate (Fig. 6.2). The bonded MoS_2, MS MoS_2, and MS DLC films generally had low coefficients of friction, low film wear rates, and low ball wear rates, similar to those for the PACVD DLC films. The wear rates of the solid

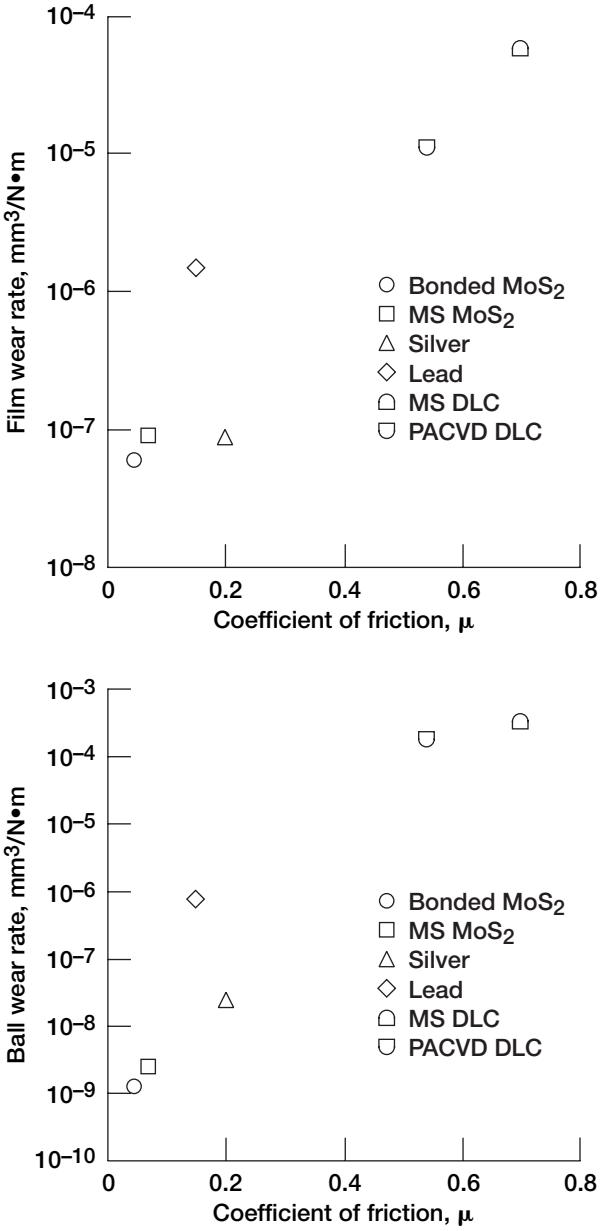

Figure 6.1.—Steady-state (equilibrium) coefficients of friction and wear rates (dimensional wear coefficients) for solid lubricating films in sliding contact with 440C stainless steel balls in ultrahigh vacuum.

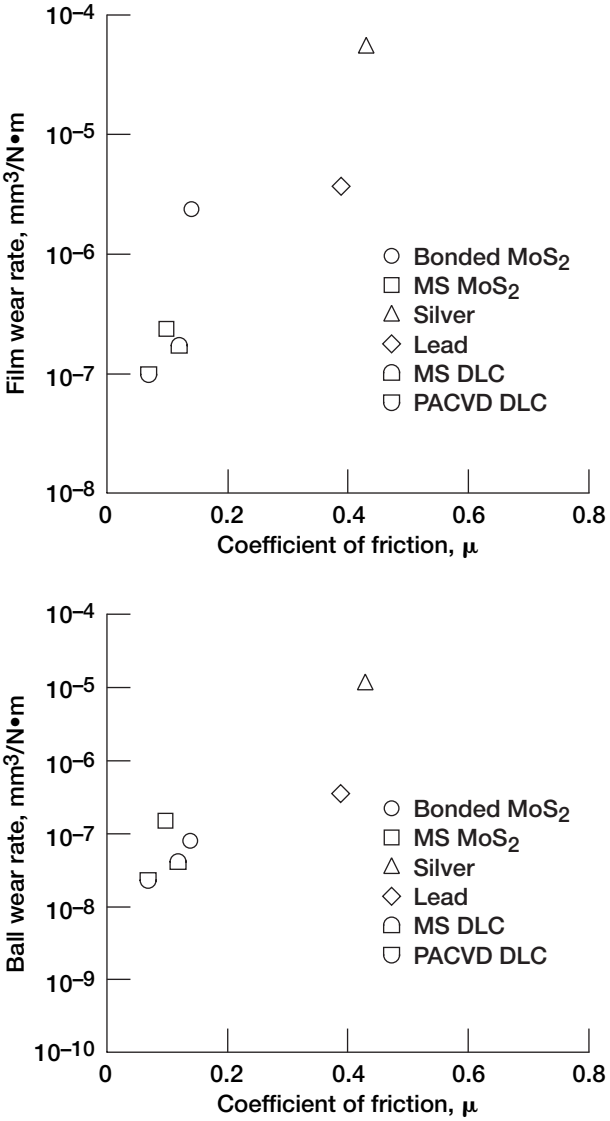

Figure 6.2.—Steady-state (equilibrium) coefficients of friction and wear rates (dimensional wear coefficients) for solid lubricating films in sliding contact with 440C stainless steel balls in humid air.

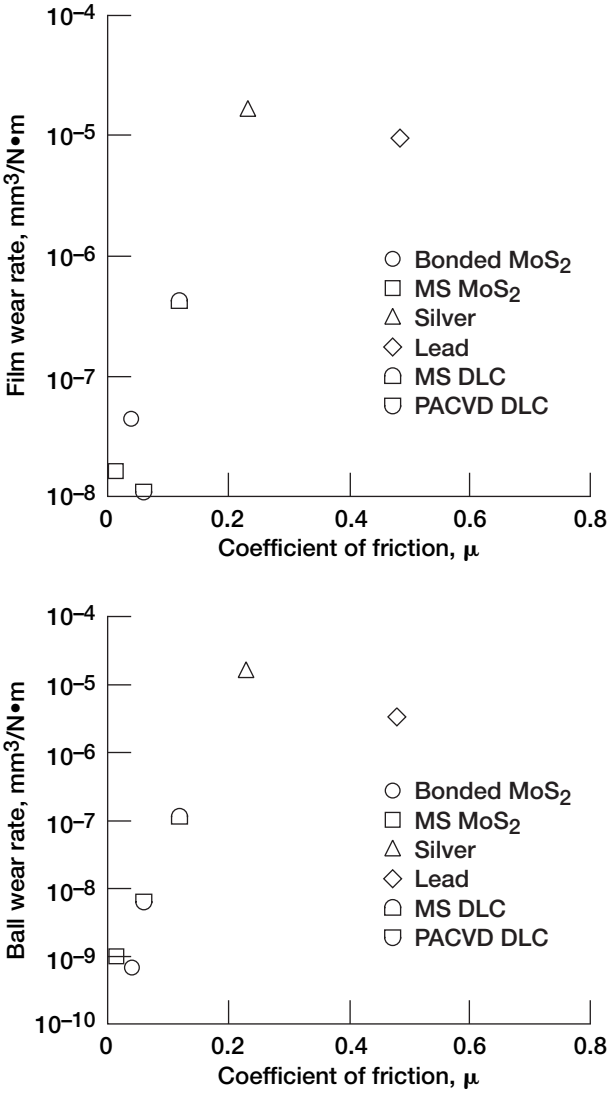

Figure 6.3.—Steady-state (equilibrium) coefficients of friction and wear rates (dimensional wear coefficients) for solid lubricating films in sliding contact with 440C stainless steel balls in dry nitrogen.

lubricating films in humid air were, in ascending order, PACVD DLC < MS DLC < MS MoS_2 < bonded MoS_2 < ion-plated lead < ion-plated silver. The coefficients of friction and the wear rates of the counterpart steel balls studied were in a similar ascending order. The ion-plated silver films had the highest coefficient of friction, highest film wear rate, and highest ball wear rate in humid air.

Dry nitrogen.—In sliding contact with 440C stainless steel balls in dry nitrogen, the MS MoS_2 films had the lowest coefficient of friction (Fig. 6.3). The bonded MoS_2, MS MoS_2, and PACVD DLC films had low coefficients of friction, low film wear rates, and low ball wear rates in dry nitrogen. However, the ion-plated silver and ion-plated lead films had high friction and high wear. The wear rates of the solid lubricating films in dry nitrogen were, in ascending order, PACVD DLC < MS MoS_2 < bonded MoS_2 < MS DLC < ion-plated lead < ion-plated silver. The coefficients of friction and wear rates of the counterpart steel balls studied were in a similar ascending order.

6.2.3 Wear Life (Endurance Life)

The sliding wear (endurance) life of the solid lubricating films deposited on 440C stainless steel disks was determined to be the number of passes at which the coefficient of friction rose to 0.30 in a given environment. As shown in Figs. 6.4 to 6.6 and Table 6.2, the sliding wear life varied with the environment and the type of solid lubricating film.

Ultrahigh vacuum.—In sliding contact with 440C stainless steel balls in ultrahigh vacuum, the bonded MoS_2 films had the longest wear life, over 1 million passes (Fig. 6.4). The wear lives of the solid lubricating films in ultrahigh vacuum were, in descending order, bonded MoS_2 > ion-plated silver > MS MoS_2 > ion-plated lead > PACVD DLC > MS DLC.

Humid air.—In sliding contact with 440C stainless steel balls in humid air, the PACVD DLC and MS DLC films had the longest wear lives, over 1 million passes (Fig. 6.5). The wear lives of the solid lubricating films in humid air were, in descending order, PACVD DLC > MS DLC > MS MoS_2 > bonded MoS_2 > ion-plated lead > ion-plated silver.

Dry nitrogen.—In sliding contact with 440C stainless steel balls in dry nitrogen, the bonded MoS_2, MS MoS_2, and PACVD DLC films had the longest wear lives, over 1 million passes (Fig. 6.6). The wear lives of the solid lubricating films in dry nitrogen were, in descending order, bonded MoS_2 > MS MoS_2 > PACVD DLC > MS DLC > ion-plated lead > ion-plated silver. The bonded MoS_2 films had wear lives of over 1 million passes in ultrahigh vacuum and dry nitrogen but only 113 570 passes in humid air. The MS MoS_2 films had wear lives of over 1 million passes in dry nitrogen, much greater than in either ultrahigh vacuum or humid air. The wear lives of the ion-plated silver films were relatively greater in ultrahigh vacuum than in either dry nitrogen or humid air.

In ultrahigh vacuum the bonded MoS_2 films had longer wear lives than the MS MoS_2 and ion-plated silver films. In humid air the DLC films had much longer

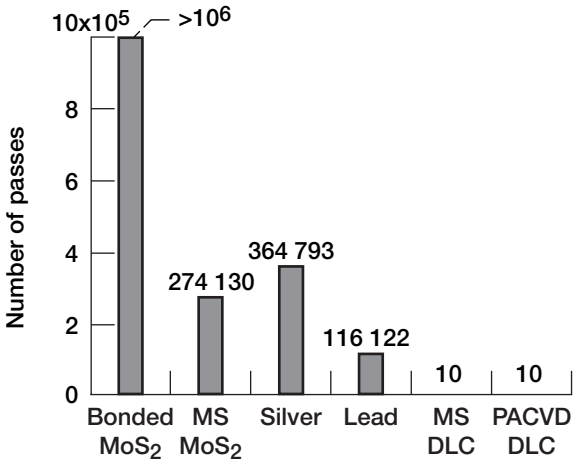

Figure 6.4.—Sliding wear lives for solid lubricating films in sliding contact with 440C stainless steel balls in ultrahigh vacuum.

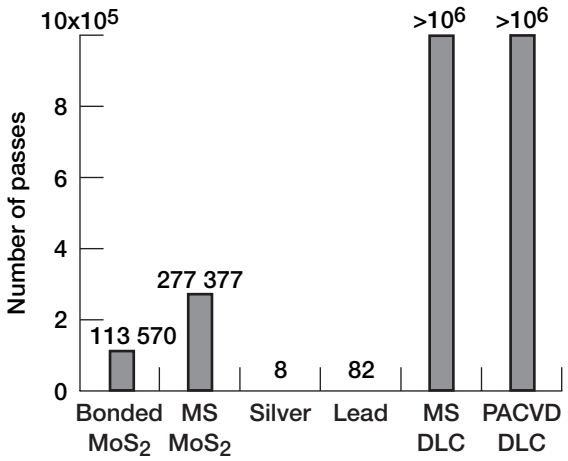

Figure 6.5.—Sliding wear lives for solid lubricating films in sliding contact with 440C stainless steel balls in humid air.

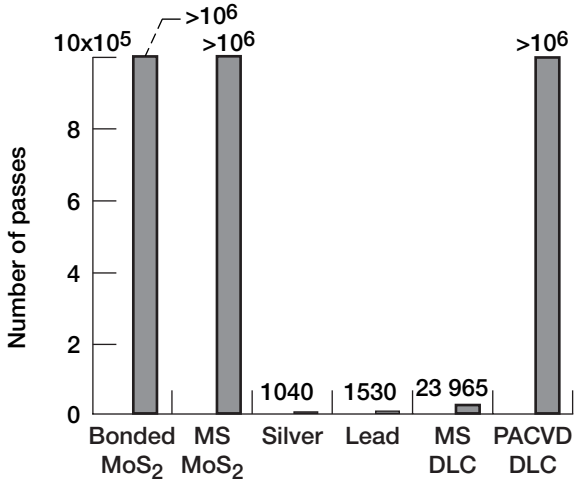

Figure 6.6.—Sliding wear lives for solid lubricating films in sliding contact with 440C stainless steel balls in dry nitrogen.

wear life than the other solid lubricating films. In dry nitrogen both the bonded MoS_2 and MS MoS_2 films had longer wear lives than the ion-plated silver films.

6.2.4 Sliding Wear Behavior, Wear Debris, and Transferred Wear Fragments

Adhesion and plastic deformation played important roles in the friction and sliding wear of the selected solid lubricating films in contact with the 440C stainless steel balls in all three environments [6.5, 6.12, 6.21]. The worn surfaces of both films and balls contained wear debris particles. Examination of the surface morphology and compositions of the worn surfaces by SEM and EDX provided detailed information about the plastic deformation of the films, wear debris, and transferred wear fragments produced during sliding. Marked plastic deformation occurred in the six solid lubricating films. Smeared, agglomerated wear debris accumulated around the contact borders, particularly on the rear ends of ball wear scars. All sliding involved adhesive transfer of materials. SEM micrographs, EDX spectra, and detailed descriptions were reported in the references [6.5, 6.12, 6.21].

Bonded MoS_2.—The 440C stainless steel balls left transferred steel fragments in the wear tracks on the bonded MoS_2 films in all three environments [6.5]. During sliding the relatively coarse asperities of the bonded MoS_2 films were deformed plastically, and the tips of the asperities were flattened under load. The ball wear scars contained transferred MoS_2 fragments. Fragments of MoS_2 and steel usually adhered to the counterpart surface or came off in loose form. Another form of adhesive MoS_2 transfer was found in sliding wear. SEM and EDX showed that a thin

MoS_2 layer (or sheet) was generated over the entire ball wear scars in all three environments.

Magnetron-sputtered MoS_2.—The 440C stainless steel balls left transferred steel fragments in the wear tracks on the MS MoS_2 films in all three environments [6.5]. The fine asperities of the sputtered MoS_2 films were flattened and elongated in the sliding direction by plastic deformation, revealing a burnished appearance. The ball wear scars contained transferred MoS_2 fragments and were entirely covered by a thin MoS_2 layer.

According to the elemental concentrations, in ultrahigh vacuum, humid air, and dry nitrogen much less transfer occurred between the films and the balls and vice versa with MS MoS_2 than with bonded MoS_2. A thin MoS_2 layer was generated over the entire ball wear scars in humid air and dry nitrogen.

Ion-plated silver.—The 440C stainless steel balls left a small amount of transferred steel fragments in the wear tracks on the ion-plated silver films in all three environments [6.5]. The fine asperities of the ion-plated silver films were flattened and elongated in the sliding direction by plastic deformation, revealing a burnished appearance. Severe plastic deformation and shearing occurred in the silver films during sliding.

According to the elemental concentrations, after sliding in ultrahigh vacuum the entire ball wear scar contained thick transferred layers (or sheets) of silver, and plate-like silver particles were deposited at the edges of the film wear track. In contrast, after sliding in humid air the ball wear scar contained an extremely small amount of transferred silver particles. This result suggests that oxidation of silver during sliding in humid air may prevent large silver transfer. However, plate-like silver debris was deposited at the edges of the film wear track. After sliding in dry nitrogen the ball wear scar contained transferred silver plates and particles. Plate-like silver debris was deposited at the edges of the film wear track. Severe plastic deformation and shearing occurred in the silver films during sliding in dry nitrogen.

Ion-plated lead.—The 440C stainless steel balls left a small amount of transferred steel fragments in the wear tracks on the ion-plated lead films in all three environments [6.12]. The fine asperities of the ion-plated lead films were flattened and elongated in the sliding direction by plastic deformation, revealing a burnished appearance. Severe plastic deformation and shearing occurred in the lead films during sliding.

According to the elemental concentrations, after sliding in ultrahigh vacuum the entire ball wear scar contained thick transferred layers (or sheets) of lead. Plate-like lead debris was found at the edges of the film wear track. In contrast, after sliding in humid air the ball wear scar contained an extremely small amount of transferred lead particles. This result suggests that oxidation of lead, like silver oxidation, during sliding in humid air may prevent large lead transfer. However, plate-like lead debris was deposited at the edges of the film wear track in humid air. After sliding in dry nitrogen the ball wear scar contained transferred lead plates and particles, and plate-like lead debris was deposited at the edges of the film wear track.

Magnetron-sputtered DLC.—With MS DLC films sliding involved generation of fine wear debris particles and agglomerated wear debris and transfer of the worn materials in all three environments [6.21].

According to the elemental concentrations, after sliding in ultrahigh vacuum the 440C stainless steel ball left a roughened worn surface and a small amount of transferred steel fragments in the wear track on the MS DLC film. The ball wear scar contained fine steel particles and a small amount of transferred DLC fragments. The wear mechanism was that of small fragments chipping off the DLC surface.

After sliding in humid air the 440C stainless steel ball left a small amount of transferred steel fragments in the wear track on the MS DLC film. The fine asperities of the MS DLC film were flattened and elongated in the sliding direction by plastic deformation, revealing a burnished appearance. The entire ball wear scar contained transferred patches and thick transferred layers (or sheets) of MS DLC. Plate-like DLC debris was also deposited at the edges of the wear scar. Severe plastic deformation and shearing occurred in the DLC films during sliding in humid air.

After sliding in dry nitrogen the 440C stainless steel ball left an extremely small amount of transferred steel debris in the wear track on the MS DLC film. In addition, smeared, agglomerated DLC debris was deposited on the film. The fine asperities of the MS DLC film were flattened and elongated in the sliding direction by plastic deformation, revealing a burnished appearance. The ball wear scar contained transferred DLC wear debris.

Plasma-assisted, chemical-vapor-deposited DLC.—With PACVD DLC films, like MS DLC films, sliding involved generation of fine wear debris particles and agglomerated wear debris and transfer of the worn materials in all three environments [6.21].

According to the elemental concentrations, after sliding in ultrahigh vacuum the 440C stainless steel ball left smeared, agglomerated DLC debris and a small amount of transferred steel fragments in the film wear track. The ball wear scar contained fine steel particles and large smeared, agglomerated patches containing transferred DLC fragments. The wear mechanism was adhesive, and plastic deformation played a role in the burnished appearance of the smeared, agglomerated wear debris.

After sliding in humid air the 440C stainless steel ball left a small amount of transferred steel fragments in the film wear track. The fine asperities of the PACVD DLC film were flattened and elongated in the sliding direction by plastic deformation, revealing a burnished appearance. The smooth ball wear scar contained an extremely small amount of transferred DLC debris.

After sliding in dry nitrogen the 440C stainless steel ball left DLC debris, micropits, and an extremely small amount of transferred steel debris in the wear track on the PACVD DLC film. The fine asperities of the film were flattened and elongated in the sliding direction by plastic deformation, revealing a burnished appearance. The ball wear scar contained fine grooves in the sliding direction, steel debris, and a small amount of transferred DLC debris.

6.2.5 Summary of Remarks

Recently developed, commercially available, dry solid film lubricants for solid lubrication applications were evaluated in unidirectional sliding friction experiments with bonded molybdenum disulfide (MoS_2) films, magnetron-sputtered (MS) MoS_2 films, ion-plated silver films, ion-plated lead films, MS diamondlike carbon (DLC) films, and plasma-assisted, chemical-vapor-deposited DLC films in contact with AISI 440C stainless steel balls in ultrahigh vacuum, in humid air, and in dry nitrogen. The main criteria for judging the performance of the dry solid lubricating films were coefficient of friction and wear rate, which had to be <0.3 and 10^{-6} $mm^3/N{\cdot}m$, respectively. The following remarks can be made:

1. Bonded MoS_2 and MS MoS_2 films met both criteria in all three environments. Also, the wear rates of the counterpart 440C stainless steel balls met that criterion in the three environments.
2. In ultrahigh vacuum the coefficient of friction and endurance (wear) life of bonded MoS_2 films were superior to those of all the other dry solid film lubricants.
3. Ion-plated silver films met both criteria only in ultrahigh vacuum, failing in humid air and in dry nitrogen, where the film and ball wear rates were higher than the criterion.
4. Ion-plated lead films met both criteria only in ultrahigh vacuum, failing in humid air and in dry nitrogen, where the coefficients of friction were greater than the criterion. Both the lead film and ball wear rates met that criterion in all three environments.
5. MS DLC and PACVD DLC films met the criteria in humid air and in dry nitrogen, failing in ultrahigh vacuum, where the coefficients of friction were greater than the criterion.
6. Adhesion and plastic deformation played important roles in the friction and wear of all the solid lubricating films in contact with 440C stainless steel balls in the three environments. All sliding involved adhesive transfer of materials: transfer of solid lubricant wear debris to the counterpart 440C stainless steel, and transfer of 440C stainless steel wear debris to the counterpart solid lubricant.

6.3 Characteristics of Magnetron-Sputtered Molybdenum Disulfide Films

Solid lubricants must not only display low coefficients of friction but also maintain good durability and environmental stability [6.2–6.7]. The ability to allow rubbing surfaces to operate under load without scoring, seizing, welding, or other manifestations of material destruction in hostile environments is an important

lubricant property. For solid lubricating films to be durable under sliding conditions, they must have low wear rates and high interfacial adhesion strength between the films and the substrates. The actual wear rates, wear modes, and interfacial adhesion strength of solid lubricating films (e.g., MS MoS_2 films), however, are widely variable, depending on operating variables and substrate preparation. This section describes the coefficient of friction, wear rate, and endurance life for MS MoS_2 films deposited on 440C stainless steel disk substrates and slid against a 440C stainless steel bearing ball [6.22, 6.23]. The MoS_2 films produced by using a standardized process and condition were characterized and qualified, typically with a number of coupon specimens and test conditions. Aspects of practical engineering decision-making were simulated to illustrate wear mechanisms as well as surface engineering principles. Eventually, this approach will become necessary for evaluating and recommending solid lubricants and operating parameters for optimum performance.

6.3.1 Experimental Procedure

Dry, solid MoS_2 films were deposited by using a magnetron radiofrequency sputtering system and a commercially available, high-purity molybdenum disulfide target on the 440C stainless steel disks [6.22, 6.23]. Table 6.3 presents the deposition conditions. Because sputtered MoS_2 films are often nonstoichiometric, films examined in this case study were named MoS_x. Table 6.4 lists the value of x, thickness, density, surface roughness, and Vickers hardness of the standard MoS_x specimens. Some details on the MoS_x films were reported in the references [6.22, 6.23].

TABLE 6.3.—MAGNETRON RADIOFREQUENCY SPUTTERING CONDITIONS

Substrate material	440C stainless steel
Substrate centerline-average surface roughness, R_a, nm	9.0 with a standard deviation of 0.9
Substrate average Vickers microhardness at loads from 0.49 to 4.9 N, GPa	6.8 with a standard deviation of 0.08
Ion etching of substrate before deposition:	
Power, W	550
Argon pressure for 5 min, Pa (mtorr)	2.7 (20)
Target material	Molybdenum disulfide
Target cleaning:	
Power, W	900
Argon pressure for 5 min, Pa (mtorr)	2.7 (20)
Target-to-substrate distance, mm	90
Deposition conditions:	
Power, W	900
Argon pressure, Pa (mtorr)	2.7 (20)
Deposition rate, nm/min	110
Power density, W/m^2	4.9×10^4
Deposition temperature	Room temperature

In a vacuum environment sputtering with rare gas ions, such as argon ions, can remove contaminants adsorbed on the surface of materials and etch the surface. The ion-sputtered surface consisted of sulfur, molybdenum, and small amounts of carbon and oxygen (see Fig. 2.33 in Chapter 2).

AES analysis provided elemental depth profiles for the MoS_x films deposited on the 440C stainless steel substrates. For example, Fig. 2.34 in Chapter 2 presented a typical example of an AES depth profile, with concentration shown as a function of the sputtering distance from the MoS_x film surface. The concentrations of sulfur and molybdenum at first rapidly increased with an increase in sputtering distance, and the concentrations of carbon and oxygen contaminant decreased. All elements remained constant thereafter. The deposited films contained small amounts of carbon and oxygen at the surface and in the bulk and had a sulfur-to-molybdenum ratio of ~1.7 (also, see Table 6.4). The relative concentrations of various constituents were determined from peak height sensitivity factors [6.24]. The MoS_x films were exposed to air before AES analysis.

Figures 6.7(a) and (b) present atomic ratios of sulfur to molybdenum (S/Mo) for thin (~110 nm thick) and thick (~1 μm thick) MoS_x films, respectively. All films were nonstoichiometric and were deposited at various laboratories in Europe and the United States by sputtering, except one of the thick films, for which a laser ablation technique was used. All the thin and all the thick sputtered MoS_x films showed approximately the same S/Mo ratios, 1.6 to 1.8 and 1.3 to 1.5, respectively. The S/Mo for two thin films deposited at the same laboratory were virtually identical and agreed well with the S/Mo obtained by Rutherford backscattering spectrometry. The laser-ablated film seemed to be more like bulk molybdenite, and the sulfur seemed to be depleted by preferential sputtering to a much greater degree ($x < 1.5$). The concentrations of carbon and oxygen contaminants (≤5 and ~2%, respectively)

TABLE 6.4.—CONDITIONS OF BALL-ON-DISK SLIDING FRICTION EXPERIMENTS

Load, N	0.49 to 3.6
Disk rotating speed, rpm	120
Track diameter, mm	5 to 17
Sliding velocity, mm/s	31 to 107
Vacuum pressure, Pa (torr)	10^{-7} (10^{-9})
Ball material	440C stainless steel (grade 10)
Ball diameter, mm	6
Ball centerline-average surface roughness, R_a, nm	6.8 with a standard deviation of 1.8
Ball average Vickers microhardness at loads from 0.49 to 4.9 N, GPa	8.7 with a standard deviation of 0.17
Disk material	Magnetron-sputtered MoS_x film on 440C stainless steel substrate
Value of x in MoS_x	1.7
Nominal film thickness, nm	110
Film density, g/cm^3	4.4
Film centerline-average surface roughness, R_a, nm	18.9 with a standard deviation of 5.9
Disk average Vickers microhardness at loads from 0.49 to 4.9 N, GPa	6.8 with a standard deviation of 0.14

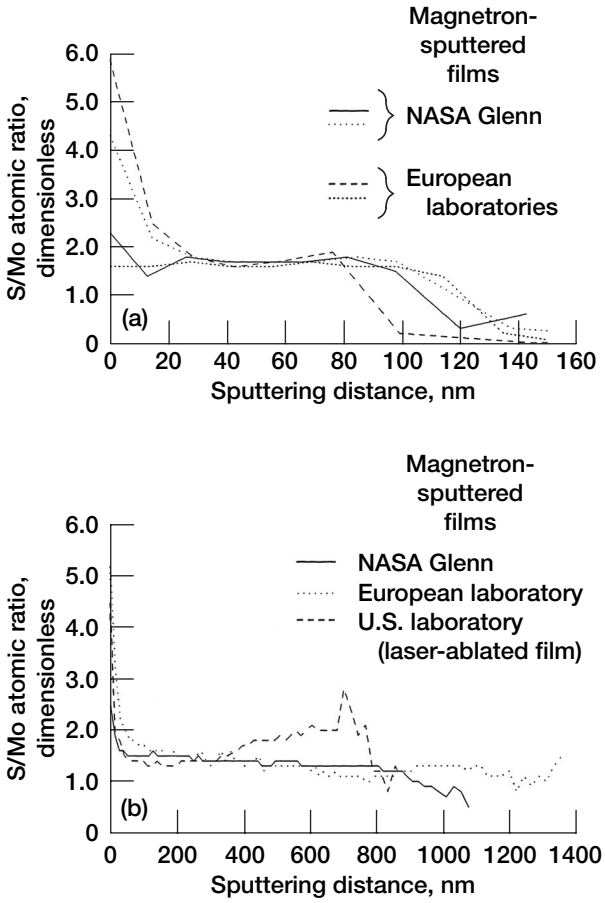

Figure 6.7.—Sulfur/molybdenum atomic ratios of MoS_x films on 440C stainless steel deposited in Europe and the United States. (a) Thin film. (b) Thick film.

in the laser-ablated MoS_x film were much less than those (≤5 to 15% and ≤10 to 25%, respectively) in the two virtually identical sputtered MoS_x films.

The average Vickers microhardness values for MoS_x films deposited on 440C stainless steel disks were ~10% lower than those for uncoated 440C stainless steel disks in the load range 0.1 to 0.25 N (Fig. 6.8). At higher loads, 1 to 5 N, however, the microhardness values for the coated disks were ~6.8 GPa, the same as those for the uncoated disks.

The surface morphology, surface roughness, and microstructure of the MoS_x films were investigated by scanning electron microscopy (SEM), surface

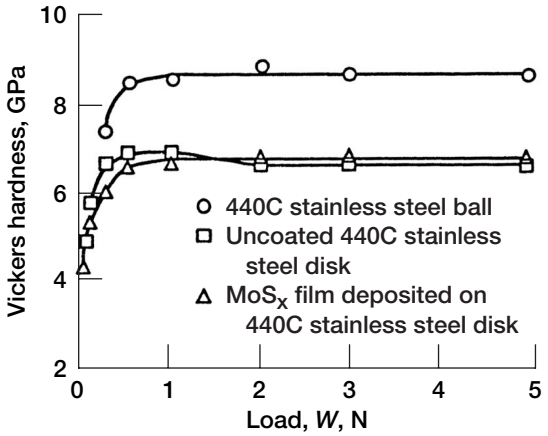

Figure 6.8.—Vickers microhardnesses as a function of load for MoS_x films on 440C stainless steel.

profilometry, and x-ray diffraction (XRD). The film surface took on a highly dense, smooth, featureless appearance. The centerline-average surface roughness R_a was 18.9 nm with a standard deviation of 5.9 nm. An x-ray diffraction pattern showed no evidence that the film had a crystalline structure. It was either amorphous or too thin (~110 nm thick), or the crystal domain size was beyond the limits of detection using XRD.

6.3.2 Friction Behavior and Endurance Life

Figures 6.9 and 6.10 present typical coefficients of friction for MoS_x films, 0.11 μm thick, deposited on sputter-cleaned 440C stainless steel disks as a function of the number of passes. Figure 6.9 extends only to 400 passes, the initial run-in period. In Fig. 6.10, the plots extend to the endurance life, the number of passes at which the coefficient of friction rose rapidly to a fixed value of ~0.15.

Quantitatively, the coefficient of friction usually started relatively high (point A) but rapidly decreased and reached its minimum value of ~0.01 (point B), sometimes decreasing to nearly 0.001 after 40 to 150 passes. Afterward, the coefficient of friction gradually increased with an increasing number of passes, as shown in Fig. 6.9. It reached its equilibrium value at point C in Fig. 6.10. From point C to point D it remained constant for a long period. At point D the coefficient of friction began to decrease and remained low from point E to point F. Finally, the sliding action caused the film to break down, whereupon the coefficient of friction rose rapidly (line F–G). The plots of Fig. 6.10 reveal the similarities in the friction behavior of MoS_x films regardless of the load applied. This evidence suggests that increasing the load may not affect the wear mode and behavior of MoS_x films.

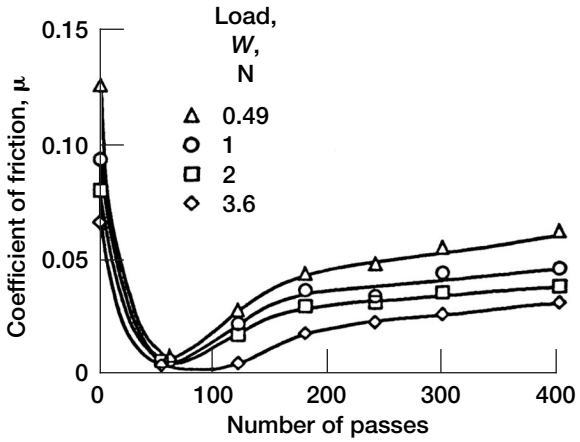

Figure 6.9.—Run-in average coefficients of friction as a function of number of passes for MoS_x films on 440C stainless steel disks in sliding contact with 440C stainless steel balls in ultrahigh vacuum.

6.3.3 Effects of Load on Friction, Endurance Life, and Wear

Friction.—The friction data presented in Figs. 6.9 and 6.10 clearly indicate that the coefficient of friction for steel balls in sliding contact with MoS_x films varies with load. In general, the higher the load, the lower the coefficient of friction. Therefore, the coefficients of friction as a function of load for the regions designated in Figs. 6.9 and 6.10 were replotted in Fig. 6.11 on logarithmic coordinates. The logarithmic plots reveal a generally strong correlation between the coefficient of friction in the steady-state condition (C–D region) and load. The relation between coefficient of friction μ and load W is given by $\mu = kW^{-1/3}$, which expression agrees with the Hertzian contact model [6.25–6.29]. Similar elastic contact and friction characteristics (i.e., load-dependent friction behavior) can also be found for bulk materials like polymers [6.25, 6.30], diamond [6.30], and ceramics [6.31], as well as for thin solid lubricants like sputtered molybdenum disulfide and ion-beam-deposited boron nitride coatings [6.32–6.35].

This load-dependent (i.e., contact pressure dependent) friction behavior allows the coefficient of friction to be deduced from the design concept (e.g., the component design parameters). Further, a better understanding of the mechanical factors controlling friction, such as load (contact pressure), would improve the design of advanced bearings and the performance of solid lubricants.

Endurance life.—Figure 6.12 presents the endurance lives of the MoS_x films as a function of load. Even in very carefully controlled conditions, repeat determinations of endurance life can show considerable scatter. Although the endurance lives

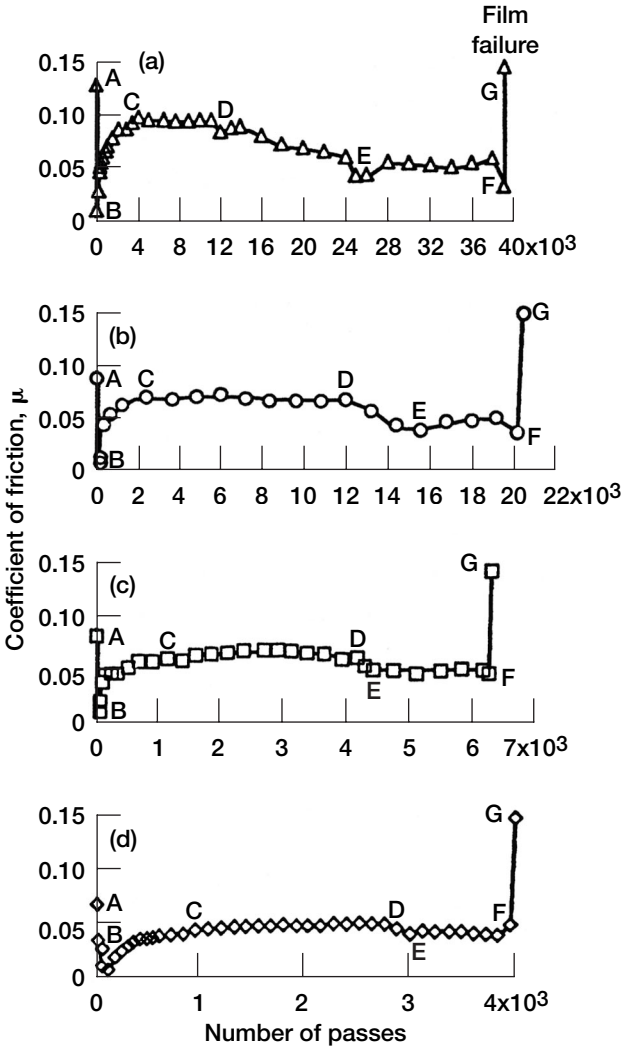

Figure 6.10.—Coefficients of friction as a function of number of passes for MoS_x films on 440C stainless steel disks in sliding contact with 440C stainless steel balls in ultrahigh vacuum. (a) Load, 0.49 N. (b) Load, 1 N. (c) Load, 2 N. (d) Load, 3.6 N.

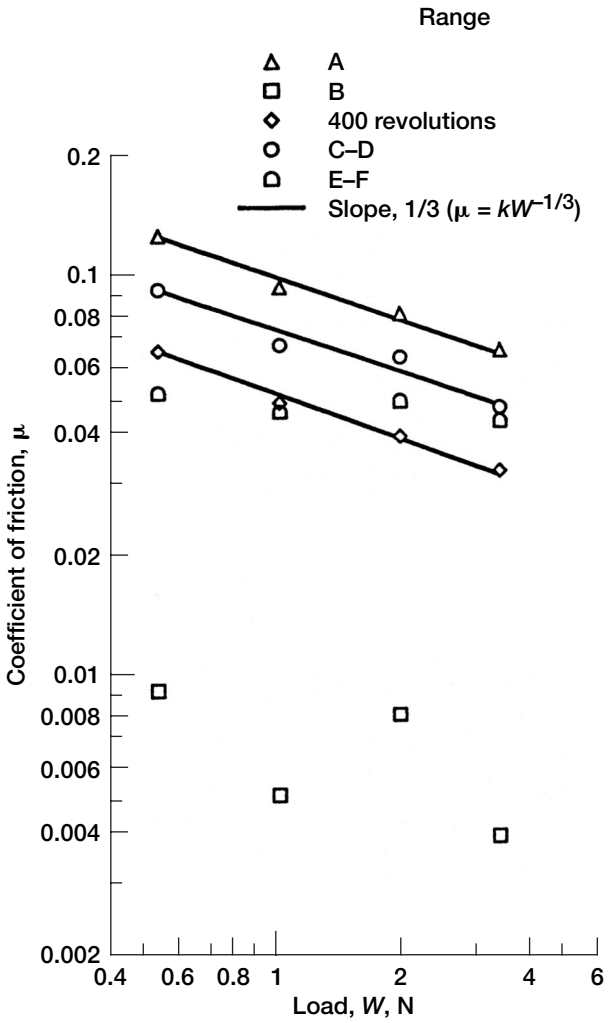

Figure 6.11.—Relation of coefficient of friction and number of passes (from regions denoted in Figs. 6.9 and 6.10) to load for MoS_x films on 440C stainless steel disks.

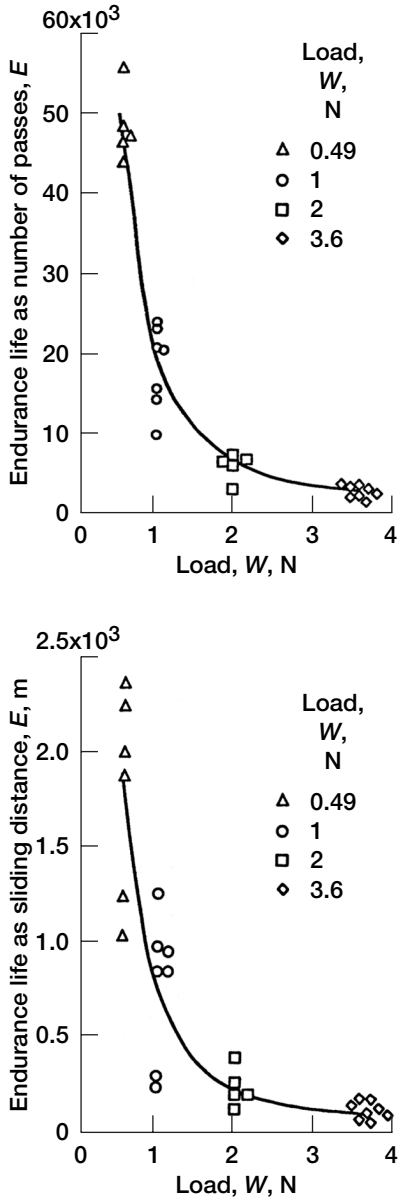

Figure 6.12.—Endurance lives as a function of load for MoS_x films on 440C stainless steel disks in sliding contact with 440C stainless steel balls in ultrahigh vacuum; Cartesian plot.

determined by the sliding distance showed larger variation than those determined by the number of passes, the trends are similar; that is, the endurance lives of MoS_x films decreased as the load increased.

To express the relation between endurance life and load empirically, the endurance life data of Fig. 6.12 were replotted on logarithmic coordinates in Fig. 6.13. A straight line was easily placed through the data in both plots of Fig. 6.13, once again revealing the strong correlation. To a first approximation for the load range investigated, the relation between endurance life E and load W on logarithmic coordinates was expressed by $E = KW^n$, where K and n are constants for the MoS_x films under examination and where the value of n was ~1.4. The load-dependent (i.e., contact pressure dependent) endurance life allows a reduction in the time needed for wear experiments and an acceleration of life testing of MoS_x films.

Specific wear rates and wear coefficients.—An attempt to estimate average wear rates for MoS_x films was made with the primary aim of generating specific wear rates and wear coefficient data that could be compared with those for other materials in the literature. It is recognized that the contact by the ball tip is continuous and that the contact by any point on the disk track is intermittent. A fundamental parameter affecting film endurance life is the number of compression and flexure cycles (intermittent contacts) to which each element of the film is subjected. Therefore, normalizing the disk wear volume by the total sliding distance experienced by the ball is fundamentally incorrect. To account for the intermittent and fatigue aspects of this type of experiment, the volume worn away should be given by

$$\text{Wear volume} = c_1 \times \text{Normal load} \times \text{Number of passes} \tag{6.1}$$

where the dimensional constant c_1 is an average specific wear rate expressed in cubic millimeters per newton·pass. However, a great quantity of historical ball-on-disk or pin-on-disk results have been reported using an expression of the form

$$\text{Wear volume} = c_2 \times \text{Normal load} \times \text{Sliding distance} \tag{6.2}$$

where the dimensional constant c_2 is an average specific wear rate expressed in cubic millimeters per newton·meter. Also, a Holm-Archard relationship is the type

$$\text{Wear volume} = c_3 \times \text{Normal load} \times \text{Sliding distance / Hardness} \tag{6.3}$$

where the nondimensional constant c_3 is the nondimensional average wear coefficient reported in the references [6.36–6.39].

Figure 6.14 presents the two specific wear rates and the wear coefficient as a function of load. That they are almost independent of load for the loads investigated suggests that increasing the load in the range 0.49 to 3.6 N may not affect the wear mode of MoS_x films.

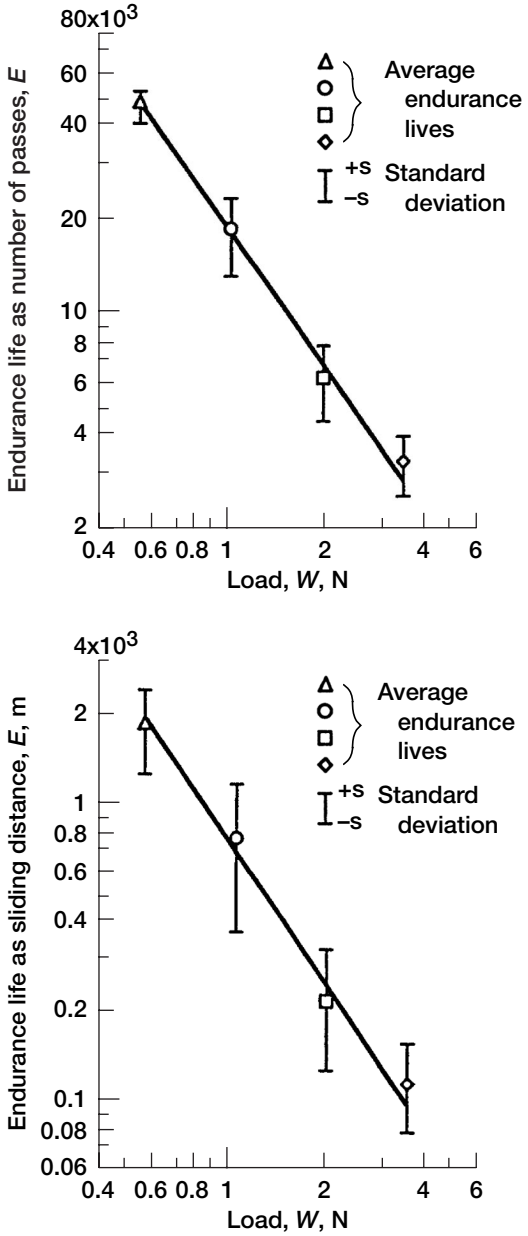

Figure 6.13.—Endurance lives as a function of load for MoS_x films on 440C stainless steel disks in sliding contact with 440C stainless steel balls in ultrahigh vacuum; logarithmic plot.

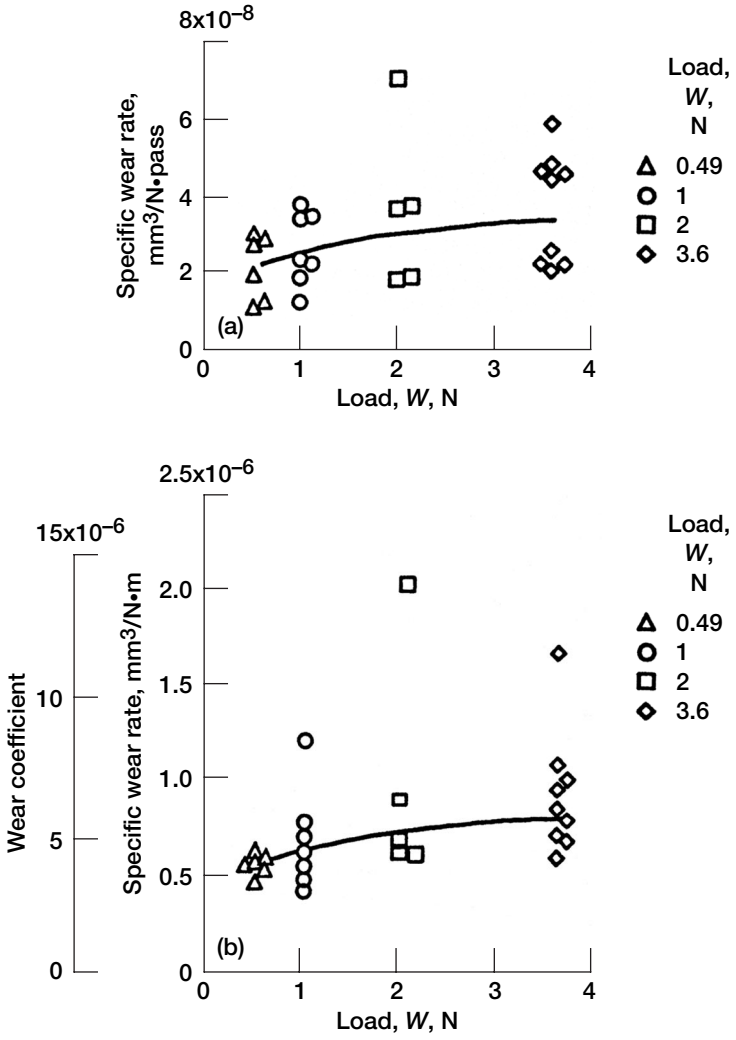

Figure 6.14.—Wear rates as a function of load for MoS_x films on 440C stainless steel disks in sliding contact with 440C stainless steel balls in ultrahigh vacuum. (a) Specific wear rate, 3×10^{-8} $mm^3/N\cdot pass$, and dimensional constant, c_1; (b) specific wear rate, 8×10^{-7} $mm^3/N\cdot m$, and dimensional constant, c_2; nondimensional wear coefficient, 5×10^{-6}, and nondimensional constant, c_3.

The worn surfaces of the MoS_x films took on a burnished appearance, and a low-wear form of adhesive wear, namely burnishing wear, was encountered. The two average specific wear rates and the nondimensional wear coefficient for the MoS_x films studied herein were ~3×10^{-8} mm^3/N·pass (c_1 in Eq. (6.1) and Fig. 6.14(a)), 8×10^{-7} mm^3/N·m (c_2 in Eq. (6.2) and Fig. 6.14(b)), and 5×10^{-6} (c_3 in Eq. (6.3) and Fig. 6.14(b)).

The very concept of specific wear rates and a wear coefficient implicitly assumes a linear relation between the volume of material removed and either the number of passes for the disk (flat) or the distance slid for a ball (pin). If it were true that roughly the same amount of material is removed from a disk specimen by each pass of the disk, the relation between wear volume and number of passes would be roughly linear, and the specific wear rates and wear coefficient would be meaningful. A consequence for solid lubricating films would be that a film twice the thickness of another similar film should last twice as long. However, if material were not removed from the disk (flat) at a constant rate, measuring the wear volume after a number of passes would give only the average amount of material removed per pass. The calculated wear rate in this case, being an average, would change with the number of passes completed, and doubling a solid lubricating film's initial thickness would not double the film endurance life. Also, simple compaction of the MoS_x film under load may primarily occur during running in. Afterward, burnishing wear may dominate the overall wear rate. The specific wear rates and wear coefficient for a material such as MoS_x film, therefore, should be viewed with caution.

6.3.4 Effects of MoS_x Film Thickness on Friction and Endurance Life

The coefficient of friction and endurance life of MoS_x films depend on the film thickness, as indicated in Figs. 6.15 and 6.16. The coefficient of friction reached a minimum value with an effective or critical film thickness of 200 nm. The endurance life of the MoS_x films increased as the film thickness increased. The relation between endurance life E and film thickness h is expressed by $E = 100h^{1.21}$ at a load of 1 N and by $E = 3.36h^{1.50}$ at a load of 3 N.

6.3.5 Roles of Interface Species

The interfacial region between an MoS_x film and a substrate surface determines many characteristics of the couple. These include film adhesion or adhesion strength, wear resistance, defects, interfacial fracture, compound formation, diffusion or pseudodiffusion, or monolayer-to-monolayer change. Also, the nature of the interfacial region determines the endurance life of MoS_x films. For example, Fig. 6.17 presents the endurance lives of 110-nm-thick MoS_x films deposited on 440C stainless steel substrates with three different interfacial species: argon-sputter-cleaned steel substrate surfaces, oxidized steel surfaces, and a rhodium interlayer produced on steel surfaces.

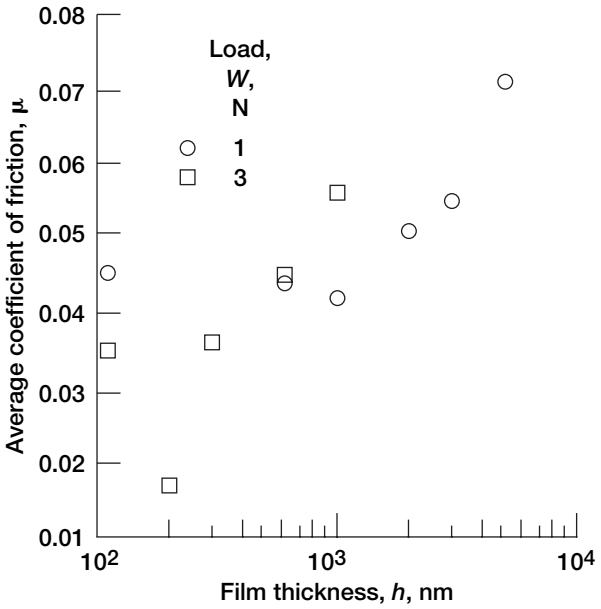

Figure 6.15.—Coefficients of friction as a function of film thickness for MoS_x films on 440C stainless steel disks in sliding contact with 440C stainless steel balls in ultrahigh vacuum.

The argon sputter cleaning and oxidation were done in situ in the deposition system just prior to the MoS_x deposition process. Argon-sputter-cleaned 440C stainless steel substrate disks were exposed to 1000 langmuirs (where 1 langmuir = 130 μPa·s (1×10^{-6} torr·s)) of oxygen (O_2) gas. The 200-, 100-, and 30-nm-thick rhodium interlayer films were produced on 440C stainless steel substrate disks by sputtering using a different deposition system. Then the rhodium-coated disks were placed in the MoS_x deposition system, the system was evacuated, and the rhodium-coated disks were argon sputter cleaned in situ just prior to the MoS_x deposition process.

Obviously, the nature and condition of the substrate surface determined MoS_x film endurance life. The oxidized substrate surface clearly led to longer life. MoS_x adhered well to the oxidized surfaces by forming interfacial oxide regions. Regardless of the interfacial adhesion mechanism the substrate surface must be free of contaminants, which inhibit interaction between the surface and the atoms of the depositing MoS_x film. The sputter-cleaned 440C stainless steel surface gave more adherent film than the rhodium surface. The rhodium metallic interlayer did not improve MoS_x adhesion. The MoS_x reacted chemically with the sputter-cleaned 440C stainless steel surface more than with the rhodium interlayer surface. The

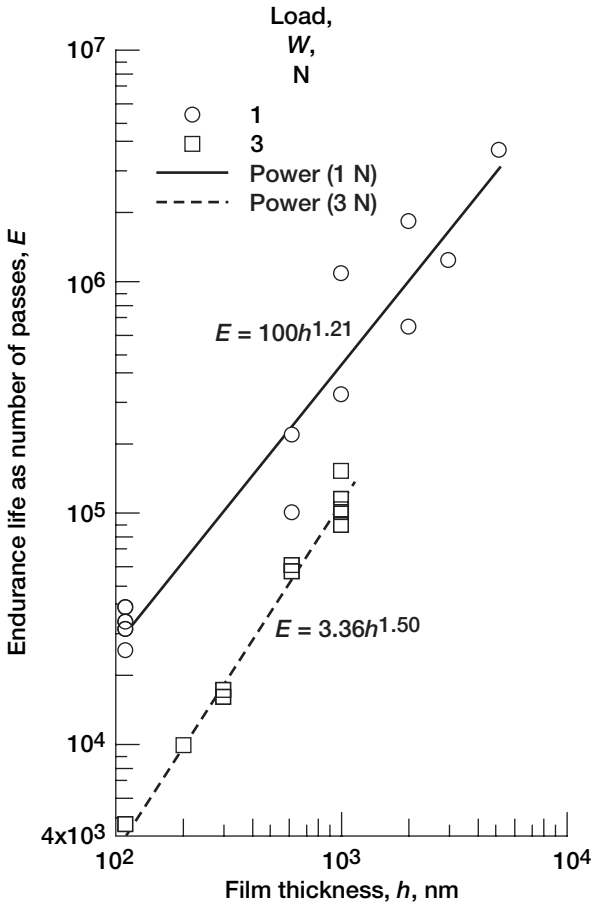

Figure 6.16.—Endurance lives as a function of film thickness for MoS_x films on 440C stainless steel disks in sliding contact with 440C stainless steel balls in ultrahigh vacuum.

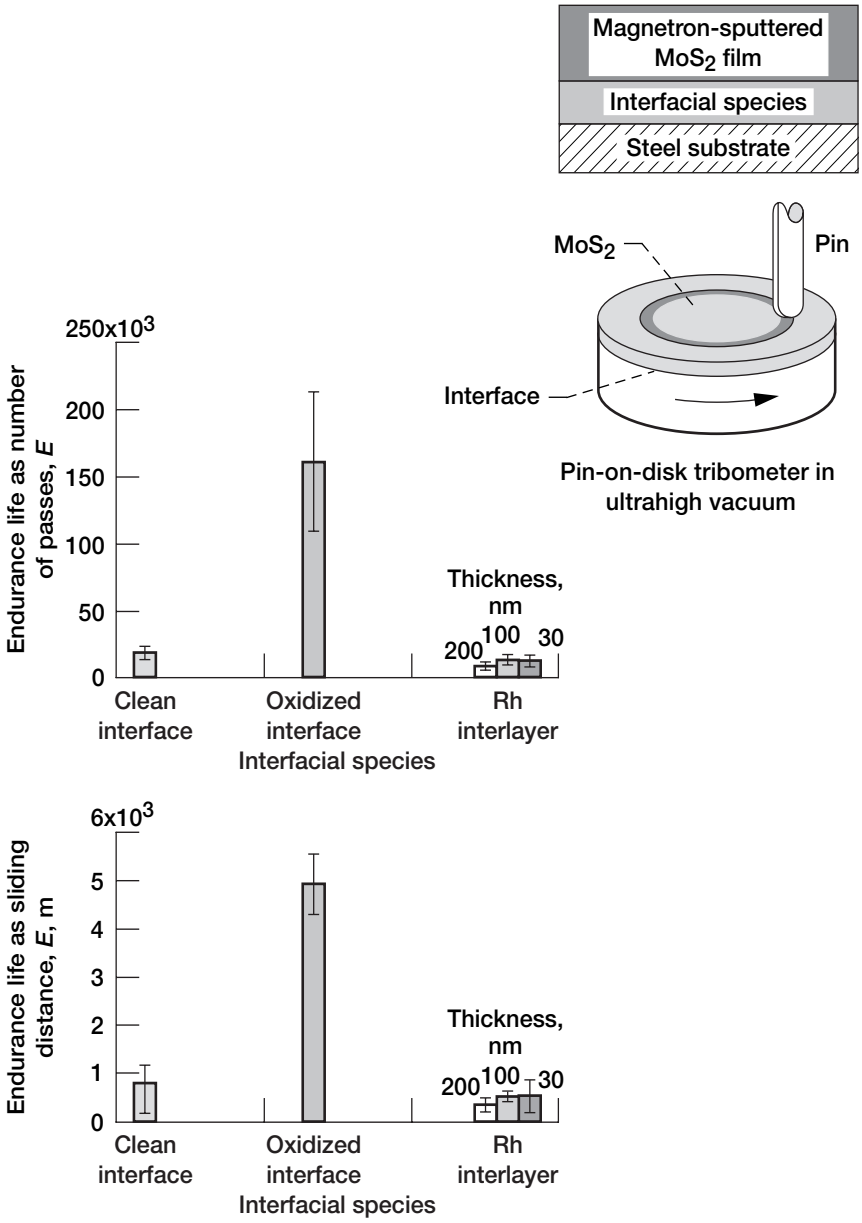

Figure 6.17.—Effect of interfacial species on endurance lives of 110-nm-thick MoS_x films on 440C stainless steel disks in sliding contact with 440C stainless steel balls in ultrahigh vacuum.

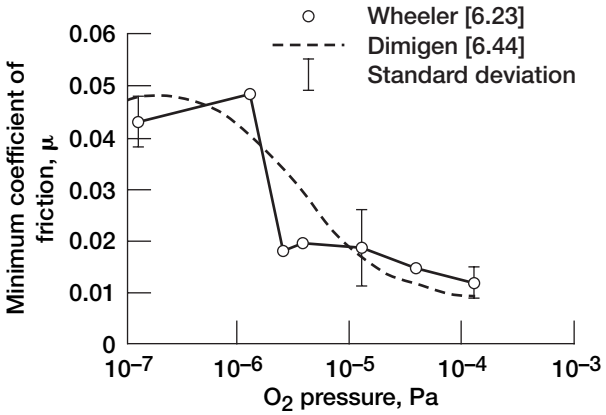

Figure 6.18.—Minimum centerline coefficients of friction as a function of oxygen pressure for 110-nm-thick $MoS_{1.7}$ films on 440C stainless steel disks in sliding contact with 440C stainless steel balls (diameter, 6 mm) at 1-N load [6.23]. The solid line connects the data points as an aid to the eye. The dashed line is the result of a similar test reported in [6.44] (see text).

thicker the rhodium interlayer, the shorter the life. However, a thin interlayer of chemically reactive metal, such as titanium or chromium, may improve adhesion.

6.3.6 Effects of Oxygen Pressure

Molybdenum disulfide is unsuitable as a dry lubricant in air because its reacts with oxygen and/or water vapor to form corrosive products [6.40, 6.41]. The ambient atmosphere in near Earth orbit consists of atomic oxygen and outgassing products from the spacecraft at pressures in the range 10^{-7} to 10^{-4} Pa [6.42, 6.43]. However, there is no evidence that these conditions are unsuitable for the use of MoS_x films. On the contrary, Dimigen et al. [6.44] observed that the coefficient of friction of magnetron-sputtered MoS_x films was substantially less when run in 10^{-6} to 10^{-4} Pa of oxygen than when run in ultrahigh vacuum (see dashed line in Fig. 6.18). Dimigen et al. measured the coefficient of friction for a range of rotational speeds and oxygen gas pressures on an $MoS_{1.4}$ film by using a pin-on-disk tribometer. The dashed line in Fig. 6.18 is an attempt to represent the results of their tests at 50 rpm. They attributed these results to an adsorption-desorption phenomenon at the sliding interface rather than to a change in the chemistry or morphology of the material itself. However, the evidence for this conclusion was not clear, and the investigation of the oxygen effect was only a peripheral part of that work.

Wheeler [6.23] investigated the effect of oxygen pressure further by using 110-nm-thick, magnetron-sputtered $MoS_{1.7}$ films on 440C stainless steel disks, which were the same as the thin MoS_x films described in Section 6.3.1. The coefficient of friction of the $MoS_{1.7}$ films was substantially reduced when sliding in low partial pressures of oxygen. The coefficient of friction was 0.04 to 0.05 at oxygen pressures of 1.33×10^{-6} Pa or less. When 2.66×10^{-6} Pa or more of oxygen was present during sliding, the coefficient of friction decreased gradually to 0.01 to 0.02, independent of the pressure. As can be seen from Fig. 6.18, the data obtained by Wheeler [6.23] agree substantially with the results of Dimigen et al. [6.44] at both high and low oxygen partial pressures.

Also, Wheeler [6.23] reported that static exposure to oxygen at any pressure did not affect the subsequent friction in vacuum. The wear scars with high friction were much larger than those with low friction. Wheeler proposed that oxygen reduces the friction force by influencing material transfer to the pin in such a way as to decrease the contact area. With this hypothesis a shear strength of 4.8±0.6 MPa, independent of oxygen pressure, was deduced for a representative film [6.23].

The endurance life of MoS_x films was strongly affected by gas interactions with the surface, such as the chemical reaction of the surface with a species or the adsorption of a species (physically or chemically adsorbed material). For example, Fig. 6.19 presents the endurance lives of 110-nm-thick MoS_x films in sliding contact with 440C stainless steel balls in oxygen gas at three pressures: 1×10^{-5}, 5×10^{-5}, and 1×10^{-4} Pa. The oxygen exposures at 1×10^{-5} and 5×10^{-5} Pa increased the endurance life by factors of 2 and 1.2, respectively, when compared with the average endurance life of 18 328 passes with a standard deviation of 5200 passes (the average sliding distance of 764 m with a standard deviation of 380 m) in ultrahigh vacuum at ~7×10^{-7} Pa. The oxygen exposure at 1×10^{-4} Pa provided endurance life almost the same as or slightly shorter than that in ultrahigh vacuum at ~7×10^{-7} Pa. Thus, extremely small amounts of oxygen contaminant, such as 1×10^{-5} Pa can increase the endurance life of MoS_x films.

6.3.7 Effects of Temperature and Environment

Increasing the surface temperature of a material tends to promote surface chemical reactions. Adsorbates on a material surface from the environment affect surface chemical reactions. These chemical reactions cause products to appear on the surface that can alter adhesion, friction, and wear [6.45]. For example, Fig. 6.20 presents the steady-state coefficients of friction for 110-nm-thick, magnetron-sputtered MoS_x films in sliding contact with 440C stainless steel balls in three environments (ultrahigh vacuum, air, and nitrogen) at temperatures from 23 to 400 °C. The data presented in the figure reveal the marked differences in friction resulting from the environmental conditions. The MoS_x films had the lowest coefficient of friction in the nitrogen environment over the entire temperature range. The coefficients of friction of the MoS_x films were, in ascending order, nitrogen

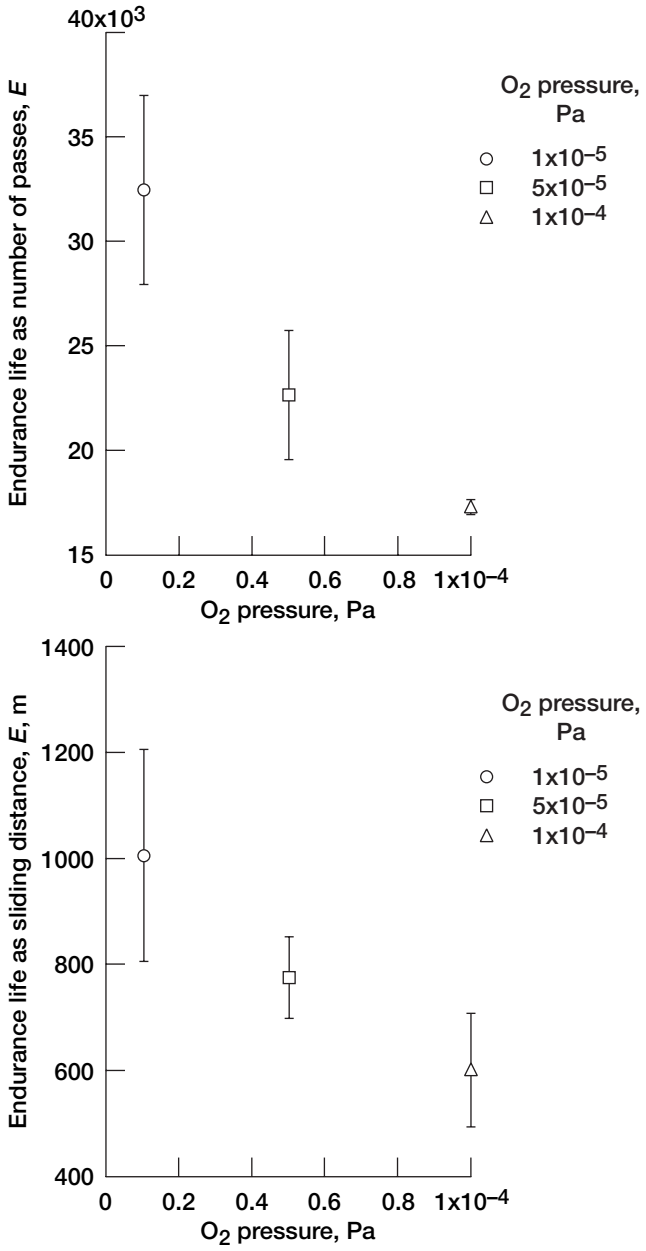

Figure 6.19.—Endurance lives as a function of oxygen pressure for 110-nm-thick MoS_x films on 440C stainless steel disks in sliding contact with 440C stainless steel balls at 1-N load.

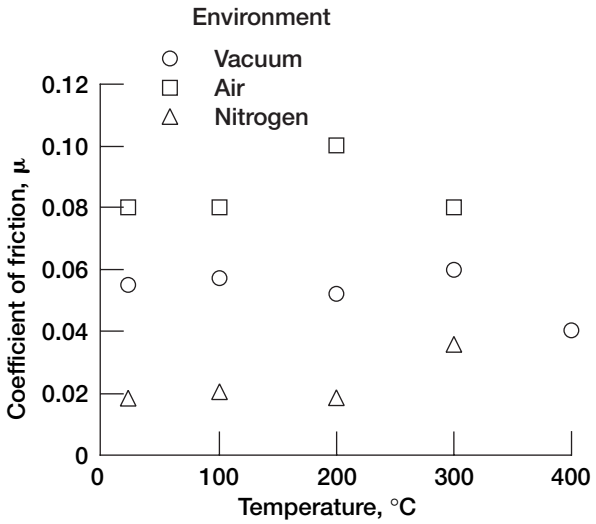

Figure 6.20.—Coefficients of friction as a function of temperature for 110-nm-thick MoS_x films on 440C stainless steel disks in sliding contact with 440C stainless steel balls in ultrahigh vacuum, humid air, and dry nitrogen.

< ultrahigh vacuum < air. Although the coefficient of friction varied with temperature, the variation was quite small.

References

6.1 H.P. Jost, Tribology—Origin and future, *Wear 136*: 1–17 (1990).

6.2 A.R. Lansdown, *Lubrication and Lubricant Selection—A Practical Guide*, Mechanical Engineering Publications, London, 1996.

6.3 M.E. Campbell, J.B. Loser, and E. Sneegas, *Solid Lubricants Technology Survey*, NASA SP–5059, 1966.

6.4 M.E. Campbell, *Solid Lubricants—A Survey*, NASA SP–5059(01), 1972.

6.5 K. Miyoshi, M. Iwaki, K. Gotoh, S. Obara, and K. Imagawa, Friction and wear properties of selected solid lubricating films, Part 1: Bonded and magnetron-sputtered molybdenum disulfide and ion-plated silver films, NASA/TM—1999-209088/PART 1, 1999.

6.6 F.J. Clauss, *Solid Lubricants and Self-Lubricating Solids*, Academic Press, New York, 1972.

6.7 J.K. Lancaster, Solid lubricants, *CRC Handbook of Lubrication: Theory and Practice of Tribology* (E.R. Booser, ed.), CRC Press, Boca Raton, FL, Vol. II, 1984, pp. 269–290.

6.8 K. Miyoshi, T. Spalvins, and D.H. Buckley, Tribological characteristics of gold films deposited on metals by ion plating and vapor deposition, *Wear 108, 2*: 169–184 (1986).

6.9 M.J. Todd and R.H. Bentall, Lead film lubrication in vacuum, *International Conference on Solid Lubrication*, SP–6, American Society of Lubrication Engineers, 1978, pp. 148–157.

6.10 J.R. Lince and P.D. Fleischauer, Solid lubrication for spacecraft mechanisms, Aerospace Corp. Report TR–97(8565)–4, 1997.

6.11 E.W. Roberts, Thin solid-lubricant films in space, *Flight-Vehicle Materials, Structures, and Dynamics* (R.L. Fusaro and J.D. Achenbach, eds.), American Society for Mechanical Engineers, New York, Vol. 4, 1993, pp. 113–132.

6.12 K. Miyoshi, M. Iwaki, K. Gotoh, S. Obara, and K. Imagawa, Friction and wear properties of selected solid lubricating films, Part 2: Ion-plated lead films, NASA/TM—2000-209088/PART 2, 2000.

6.13 H.O. Pierson, *Handbook of Carbon, Graphite, Diamond, and Fullerenes: Properties, Processing, and Applications*, Noyes Publications, Park Ridge, NJ, 1993.

6.14 J.J. Pouch and S.A. Alterovitz, eds., Properties and characterization of amorphous carbon films, *Materials Science Forum*, Trans Tech Publications, Aedermannsdorf, Switzerland, Vols. 52 & 53, 1990.

6.15 K. Miyoshi, J.J. Pouch, and S.A. Alterovitz, Plasma-deposited amorphous hydrogenated carbon films and their tribological properties, *Materials Science Forum* (J.J. Pouch and S.A. Alterovitz, eds.), Trans Tech Publications, Aedermannsdorf, Switzerland, Vols. 52 & 53, 1990, pp. 645–656.

6.16 R.L.C. Wu, K. Miyoshi, R. Vuppuladhadium, and H.E. Jackson, Physical and tribological properties of rapid thermal annealed diamond-like carbon films, *Surf. Coat. Tech. 55, 1–3*: 576–580 (1992).

6.17 K. Miyoshi, B. Pohlchuck, K.W. Street, J.S. Zabinski, J.H. Sanders, A.A. Voevodin, and R.L.C. Wu, Sliding wear and fretting wear of diamondlike carbon-based, functionally graded nanocomposite coatings, *Wear 229*: 65–73 (1999).

6.18 A.P. Molloy and A.M. Dionne, eds., *World Markets, New Applications, and Technology for Wear and Superhard Coatings*, Gorham Advanced Materials, Inc., Gorham, ME, 1998.

6.19 K. Miyoshi, M. Murakawa, S. Watanabe, S. Takeuchi, and R.L.C. Wu, Tribological characteristics and applications of superhard coatings: CVD Diamond, DLC, and c-BN, *Proceedings of Applied Diamond Conference/Frontier Carbon Technology Joint Conference 1999*, Tsukuba, Japan, 1999, pp. 268–273. (Also NASA/TM—1999-209189, 1999.)

6.20 K. Miyoshi, Diamondlike carbon films: Tribological properties and practical applications, *New Diamond and Frontier Carbon Technology 9, 6*: 381–394 (1999).

6.21 K. Miyoshi, M. Iwaki, K. Gotoh, S. Obara, and K. Imagawa, Friction and wear properties of selected solid lubricating films, Part 3: Magnetron-sputtered and plasma-assisted, chemical-vapor-deposited diamondlike carbon films, NASA/TM—2000-209088/PART 3, 2000.

6.22 K. Miyoshi, F.S. Honecy, P.B. Abel, S.V. Pepper, T. Spalvins, and D.R. Wheeler, A vacuum (10^{-9} torr) friction apparatus for determining friction and endurance life of MoS_x films, *Tribol. Trans. 36, 3*: 351–358 (1993).

6.23 D.R. Wheeler, Effect of oxygen pressure from 10^{-9} to 10^{-6} torr on the friction of sputtered MoS_x films, *Thin Solid Films 223,1*: 78–86 (1993).

6.24 L.E. Davis, N.C. MacDonald, P.W. Palmberg, G.E. Riach, and R.E. Weber, *Handbook of Auger Electron Spectroscopy*, Physical Electronics Division, Perkin-Elmer Corp., Eden Prairie, MN, 1979.

6.25 R.C. Bowers, Coefficient of friction of high polymers as a function of pressure, *J. Appl. Phys. 42, 12*: 4961–4970 (1971).

6.26 R.C. Bowers and W.A. Zisman, Pressure effects on the friction coefficient of thin-film solid lubricants, *J. Appl. Phys. 39, 12*: 5385–5395 (1968).

6.27 B.J. Briscoe, B. Scruton, and F.R. Willis, The shear strength of thin lubricant films, *Proc. R. Soc. London Ser. A 333*: 99–114 (1973).

6.28 B.J. Briscoe and D.C.B. Evans, The shear properties of Langmuir-Blodgett layers, *Proc. R. Soc. London Ser. A 380*: 389–407 (1982).

6.29 T.E.S. El-Shafei, R.D. Arnell, and J. Halling, An experimental study of the Hertzian contact of surfaces covered by soft metal films, *ASLE Trans. 26, 4*: 481–486 (1983).

6.30 F.P. Bowden and D. Tabor, *The Friction and Lubrication of Solids*, Pt. 2, Clarendon, Oxford, 1964.
6.31 K. Miyoshi, Adhesion, friction, and micromechanical properties of ceramics, *Surf. Coat. Tech. 36, 1–2*: 487–501 (1988).
6.32 S.A. Karpe, Effects of load on friction properties of molybdenum disulfide, *ASLE Trans. 8, 2*: 164–178 (1965).
6.33 I.L. Singer, R.N. Bolster, J. Wegand, S. Fayeulle, and B.C. Strupp, Hertzian stress contribution to low friction behavior of thin MoS_2 coatings, *Appl. Phys. Lett. 57, 10*: 995–997 (1990).
6.34 L.E. Pope and J.K.G. Panitz, The effects of Hertzian stress and test atmosphere on the friction coefficients of MoS_2 coatings, *Surf. Coat. Tech. 36, 1*: 341–350 (1988).
6.35 K. Miyoshi, Fundamental tribological properties of ion-beam-deposited boron nitride films, *Materials Science Forum* (J.J. Pouch and S.A. Alterovitz, eds.), Trans Tech Publications, Aedermannsdorf, Switzerland, Vols. 54 & 55, 1990, pp. 375–398.
6.36 E. Rabinowicz, Wear coefficients, *CRC Handbook of Lubrication: Theory and Practice of Tribology* (E.R. Booser, ed.), CRC Press, Boca Raton, FL, Vol. II, 1984, pp. 201–208.
6.37 R. Holm, *Electric Contacts*, Almquist & Wiksells, Stockholm, 1946, Section 40.
6.38 J.F. Archard, Contact and rubbing of flat surfaces, *J. Appl. Phys. 24, 8*: 981–988 (1953).
6.39 E. Rabinowicz, The least wear, *Wear 100, 1*: 533–541 (1984).
6.40 A.W.J. De Gee, G. Salomon, and J.H. Zatt, On the mechanisms of MoS_2-film failure in sliding friction, *ASLE Trans. 8, 2*: 156–163 (1965).
6.41 E.W. Roberts, The tribology of sputtered molybdenum disulfide films, *Friction, Lubrication, and Wear 50 Years On*, Institute of Mechanical Engineering, London, 1987, pp. 503–510.
6.42 E.W. Roberts, Ultralow friction films of MoS_2 for space applications, *Thin Solid Films 181*: 461–473 (1989).
6.43 E.W. Roberts, Thin solid lubricant films in space, *Tribol. Int. 23, 2*: 95–104 (1990).
6.44 H. Dimigen, H. Hübsch, P. Willich, and K. Reichelt, Stoichiometry and friction properties of sputtered MoS_x layers, *Thin Solid Films 129, 1*: 79–91 (1985).
6.45 C.J. Smithells, *Metals Reference Book*, 4th ed., Plenum Press, Vol. 1, 1967.

REPORT DOCUMENTATION PAGE

Form Approved
OMB No. 0704-0188

1. AGENCY USE ONLY (*Leave blank*)	2. REPORT DATE	3. REPORT TYPE AND DATES COVERED
	December 2000	Technical Memorandum

4. TITLE AND SUBTITLE

Solid Lubrication Fundamentals and Applications
Friction and Wear Properties of Selected Solid Lubricating Films: Case Studies

5. FUNDING NUMBERS

WU–505–63–5A

6. AUTHOR(S)

Kazuhisa Miyoshi

7. PERFORMING ORGANIZATION NAME(S) AND ADDRESS(ES)

National Aeronautics and Space Administration
John H. Glenn Research Center at Lewis Field
Cleveland, Ohio 44135–3191

8. PERFORMING ORGANIZATION REPORT NUMBER

E–9863-6

9. SPONSORING/MONITORING AGENCY NAME(S) AND ADDRESS(ES)

National Aeronautics and Space Administration
Washington, DC 20546–0001

10. SPONSORING/MONITORING AGENCY REPORT NUMBER

NASA TM—2000-107249/
Chapter 6

11. SUPPLEMENTARY NOTES

Responsible person, Kazuhisa Miyoshi, organization code 5140, 216–433–6078.

12a. DISTRIBUTION/AVAILABILITY STATEMENT

Unclassified - Unlimited
Subject Category: 27 Distribution: Nonstandard
Available electronically at http://gltrs.grc.nasa.gov/GLTRS
This publication is available from the NASA Center for AeroSpace Information, 301–621–0390.

12b. DISTRIBUTION CODE

13. ABSTRACT ***(Maximum 200 words)***

This chapter focuses attention on the friction and wear properties of selected solid lubricating films to aid users in choosing the best lubricant, deposition conditions, and operational variables. For simplicity, discussion of the tribological properties of concern is separated into two parts. The first part of the chapter discusses the different solid lubricating films selected for study including commercially developed solid film lubricants: bonded molybdenum disulfide (MoS_2), magnetron-sputtered MoS_2, ion-plated silver, ion-plated lead, magnetron-sputtered diamondlike carbon (MS DLC), and plasma-assisted, chemical-vapor-deposited diamondlike carbon (PACVD DLC) films. Marked differences in the friction and wear properties of the different films resulted from the different environmental conditions (ultrahigh vacuum, humid air, and dry nitrogen) and the solid film lubricant materials. The second part of the chapter discusses the physical and chemical characteristics, friction behavior, and endurance life of the magnetron-sputtered MoS_2 films. The role of interface species and the effects of applied load, film thickness, oxygen pressure, environment, and temperature on the friction and wear properties are considered.

14. SUBJECT TERMS	15. NUMBER OF PAGES
Solid lubrication; Coatings; Tribology fundamentals; Applications	42
	16. PRICE CODE: A03

17. SECURITY CLASSIFICATION OF REPORT	18. SECURITY CLASSIFICATION OF THIS PAGE	19. SECURITY CLASSIFICATION OF ABSTRACT	20. LIMITATION OF ABSTRACT
Unclassified	Unclassified	Unclassified	